https://ntrs.nasa.gov/search.jsp?R=19920010780 2020-03-17T13:24:53+00:00Z

GODDARD GRANT
IN-45-CR
75753
P-54

March 9, 1992

Regional Climate Change Predictions from the Goddard Institute for Space Studies High Resolution GCM

Crane, R.G. and Hewitson, B.C. Earth System Science Center & Dept. of Geography, The Pennsylvania State University, University Park, PA 16802

Final Report: NASA Grant NAG 5-1133
May 1989-October 1991

ABSTRACT: A new diagnostic tool is developed for examining relationships between the synoptic-scale circulation and regional temperature distributions in GCMs. The $4^{o}x5^{o}$ Goddard Institute for Space Studies (GISS) GCM is shown to produce accurate simulations of the variance in the synoptic-scale sea level pressure distribution over the United States. An analysis of the observational data set from the National Meteorological Center (NMC) also shows a strong relationship between the synoptic circulation and grid-point temperatures. This relationship is demonstrated by deriving transfer functions between a time-series of circulation parameters and temperatures at individual grid-points. The circulation parameters are derived using rotated principal components analysis, and the temperature transfer functions are based on multivariate polynomial regression models. The application of these transfer functions to the GCM circulation indicates that there is considerable spatial bias present in the GCM temperature distributions. The transfer functions are also used to indicate the possible changes in U.S. regional temperatures that could result from the differences in synoptic-scale circulation between a $1XCO_2$ and a $2xCO_2$ climate, using a doubled CO_2 version of the same GISS GCM.

(NASA-CR-190037) REGIONAL CLIMATE CHANGE PREDICTIONS FROM THE GODDARD INSTITUTE FOR SPACE STUDIES HIGH RESOLUTION GCM Final Report, May 1989 - Oct. 1991 (Pennsylvania State Univ.) 54 p CSCL 13B G3/45 N92-20022 Unclas 0075753

1. INTRODUCTION[1]

General Circulation Models (GCMs) of the atmosphere are used in a wide variety of applications in the atmospheric sciences, ranging from reconstructions of past climates to the prediction of future climate change. The current generation of these models includes a realistic geography, interactive clouds, terrestrial vegetation and hydrology, polar sea ice, and, to a greater or lesser degree, some dynamic or thermodynamic interaction with the ocean surface. Despite differences in numerical methods, parameterization schemes, and grid box resolution, all of the models do a reasonable job of simulating the large-scale features of the climate system (Schlesinger and Mitchell, 1987). This level of treatment has proved very useful in reconstructing past climates (see, for example, work by Barron and Washington, 1984) and provides considerable insight into the workings of the present day atmosphere. Furthermore, model simulations of global climate change are seen as an essential component of any program aimed at understanding human impacts on the global environment (National Academy of Sciences, 1986). In this respect, all of the recent GCM predictions of CO_2 induced warming show similar results when averaged annually and over a hemisphere. Where the models tend to show large disagreement, however, is in their regional-scale predictions of climate change. The few model intercomparison studies that have been undertaken (eg. National Research Council, 1983; Schlesinger and Mitchell, 1987; Grotch and MacCracken, 1991) all indicate that the models do a relatively poor job of simulating the atmosphere over less than the monthly-averaged hemispheric time and space scales; however, society's ability to plan for environmental change will be dictated largely by the degree to which it can predict the regional impacts of future climates. A major problem thus exists when moving from the glo-

1. The material presented here has been previously published as Hewitson and Crane (1992a; 1992b). Further details can be found in Hewitson (1990; 1991).

bal scale where current GCMs work best, to the regional and local scale (i.e. sub-continental and river basin scales) where climate change predictions are necessary for impact assessment.

Feedbacks and interactions in the climate system operate over a variety of temporal and spatial scales, such that it is difficult to treat any single component of the system in isolation. For large areas of the extra-tropics, however, numerous studies have demonstrated that the synoptic atmospheric circulation is a major factor influencing short-term climate variability at the regional and local scale. Crane (1978, 1979), for example, shows that regional and interannual variations in Arctic sea ice cover can be attributed to differences in the frequency of occurrence of particular synoptic circulation patterns. Similar studies for parts of North America again show strong relationships between circulation and regional climate, with specific patterns of atmospheric circulation giving rise to characteristic precipitation and temperature anomalies (eg. Klein and Klein, 1984; 1986; Yarnal and Diaz, 1986).

An analysis of a GCM's synoptic-scale circulation is of interest, therefore, for several reasons. First, it demonstrates how well the model simulates the small-scale variability that is averaged to produce the longer-term patterns more usually reported in GCM studies, and, second, it may be of great significance for the regional-scale interpretation of GCM output. If current GCMs can be shown to have sufficient resolution to infer sub-continental scale climate anomalies, this would raise the possibility that the model could be used to derive information on regional climate, or climate-related parameters, through the use of meso-scale models, or through empirical analyses of observed circulation-climate relationships. Work by Giorgio (1990), for example, indicates that a meso-scale model embedded within a GCM (i.e. driving the meso-scale model with boundary conditions set by the GCM) can significantly improve the regional-scale climate distribution. In the long run, this approach may

prove to be the optimum for regional climate analysis. At present, however, this method still faces the problem that the model is being driven by a small number of individual GCM grid-points, using climate values that have a large degree of error. This report focuses on the second approach, addressing the question of the representativeness of the GCM output at the regional scale by examining the daily synoptic-scale atmospheric circulation simulated by the Goddard Institute for Space Studies (GISS) GCM over the United States. Few studies have focused on the synoptic circulation in GCMs, although Crane and Barry (1988) have looked at the Arctic circulation, and Bates and Meehl (1986) have examined the geographic distribution of blocking in the NCAR Community Climate Model. In this report we describe a methodology developed for validating the model's synoptic-scale circulation, and we compare the temporal and spatial variability of observed synoptic-scale events in the National Meteorological Center (NMC) sea level pressure data set with the circulation simulated by the control run of the GISS (4^{o} x 5^{o}) GCM. We then demonstrate that the synoptic circulation also explains a substantial proportion of the surface air temperature variance over the United States. The final part of the report explores a method for combining this empirical information with GCM output to assess possible regional-scale CO_2-induced temperature change. It should be emphasized that the objective of the paper is not to provide a descriptive "synoptic climatology" of the GCM, rather the objective is to validate the short-term variability in the model circulation in order to determine the possible utility of the model for regional-scale climate assessment. The GISS model is chosen because, at the time that the analysis was carried out, it was the highest resolution model available for which we were able to obtain several years of daily data.

2. *DATA PREPARATION*

Data Characteristics:

Daily (1200z) National Meteorological Center (NMC) gridded data, and 1200z grids from a control run of the 4^{o} x 5^{o} GISS GCM Model II, are used to validate the simulated synoptic-scale atmospheric circulation. Hansen et al. (1983) describe the structure, equations, and parameterizations of the GISS model, which is global in horizontal extent and has variable vertical resolution. The model run used here has 9 layers in the vertical with a distribution of two in the boundary layer, five in the rest of the troposphere, and two in the stratosphere. The top of the model atmosphere is fixed at 10mb. The model considers the radiative heating and the transfers of energy, mass, and momentum, both horizontally and vertically. Large-scale and convective cloud parameterizations are included, as are ground processes, and ground-atmosphere interactions through the surface air layer. Snowcover may occur over land or ice as dictated by the model, and surface-atmosphere interactions are dependent on surface type. The cloud cover is given as a fraction of each grid box for each layer, and the ocean ice cover and the sea surface temperatures are specified climatologically. Further descriptions of the model, and model sensitivities, are given in Hansen et al. (1984), and Rind (1988). The spatial coverage used in the present study bounds the continental United States from 125^{o}W to 70^{o}W, and from 26^{o}N to 50^{o}N, the limits being prescribed by the GISS supplied data. The model is run out to an equilibrium state, and the analysis described here uses two years, following equilibrium, of the model control run with 1950s atmospheric CO_2 levels, and the only model parameter used is the model's sea level pressure field.

The observed data are obtained from an NMC gridded data product available at NCAR. The NMC analysis technique takes station surface and upper air data and derives an internally consistent set of gridded products for use in the NMC forcast model. The analysis described here uses the

sea level pressures and surface air temperatures from this data set that have been extrapolated to a grid of nominally equidistant points overlain on a polar stereographic projection (Jenne, 1975). Our analysis uses daily data from 1960 to 1974, the length of record being determined partly by computing constraints and partly by the increased incidence of missing data that occurs in the latter 1970s. The NMC analysis methods employed during the 1960s and early 1970s underwent few changes, and are essentially those described by Cressman (1959). The changes that did occur involved the addition of new variables, some minor improvements to the algorithms, and the porting of the model to new computer systems. The observed errors are limited primarily to boundary problems and to data sparse areas, neither of which affect the region used here.

Data Pre-processing:

The data pre-processing consisted of filling in missing days in the NMC data, interpolating the GISS grid to the NMC grid, and removing the seasonal cycle from both data sets. The data gaps in the NMC record were of one day duration except for a single case with two missing days; consequently, linear interpolation between the previous and the following day's values are used to fill in missing grids. Missing days comprised only 27 days out of the 15 year period.

The GISS model operates on a longitude-latitude grid that results in a longitudinal difference of up to 30% in the distance between grid points from the southern to the northern boundaries of the region. This biases the data matrix to the northern part of the grid, and the GISS data are thus interpolated to the NMC grid prior to analysis. The potential error introduced by interpolation is examined by re-interpolating the grid-point values back to the original GISS grid, subtracting the re-interpolated field from the original, and dividing by two. This was done for each grid point and for every day in the series. The mean and the standard deviation of the differences were calculated at each grid point, and range from -0.64

mb to +0.66 mb for the mean differences, and 0.0 mb to 1.62 mb for the standard deviations (the mean and standard deviation averaged over all grid points was -.02 mb and 0.75 mb).

The interpolation increases the number of grid points for the GISS data from 84 to 126 (Figure 1). Mapping the data to a common grid has the

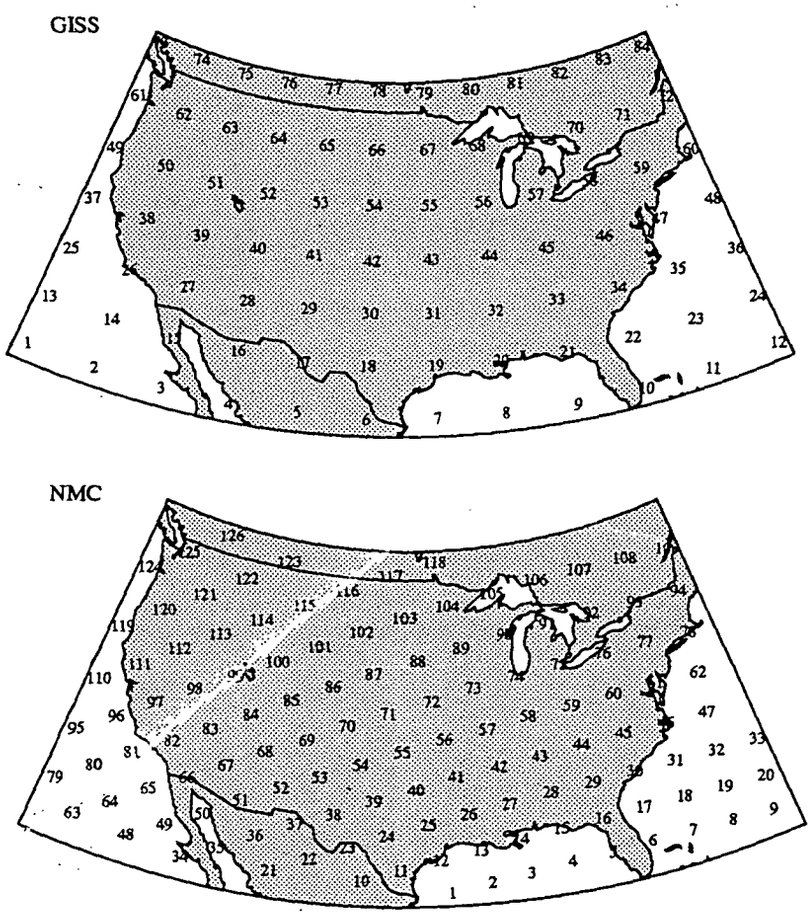

FIGURE 1. Distribution of Grid-Points in the NMC and GISS Data Sets

further advantage of facilitating the comparison of the two data sets. The interpolation algorithm used is, in essence, an implementation of the equations presented by Willmott et al. (1985). The routine searches for N number of grid points within a pre-selected radius of the location of the interpolated point. The spherical distance to each point is calculated, and the points are weighted according to the inverse square of their distance from the point to be interpolated. Any directional bias is removed by adjusting the weights according to the angular separation between the points. A feature presented by Willmott et al. (1985) that allowed an interpolated point to be projected beyond the range of the data set was excluded in order to preserve a conservative approach to the study.

The objective of the study is to isolate and compare the primary modes of the synoptic-scale atmospheric circulation in the model and the NMC data, that have temporal characteristics of days-to-weeks. Consequently, it is necessary to remove all components of the variance within the data set with time scales longer than the synoptic events of interest. This was achieved using a simple moving average filter with a 13-day cutoff, centered on the day concerned. Each grid point is expressed as the difference from a mean value, where the mean is the average of all grid points over the 13 days. This procedure removes 6 days from the beginning and end of both data sets, which amounts to 0.2% of the NMC data and 1.6% of the model grids. The 13-day filter was selected based on autocorrelation (correlograms) and power spectra of sea level pressure time series at a range of grid points. The power spectra indicate the spectral peaks, and the correlogram shows where significant autocorrelation exists. It is assumed that harmonics occur where peaks in the power spectrum match peaks in the correlogram. The filter time period was then set at the period just prior to the first significant harmonic. While several grid points showed the first major harmonic occurring at about 8 days, all showed a harmonic at about 14 days (which was also the first or second harmonic in each case) hence the 13-day filter.

Principal Components Analysis:

Principal Components Analysis (PCA) is used to characterize the primary modes of spatial and temporal variability in the observed and simulated climate, and the model validation is based on correlations between the component loadings for the two sets, and on a time series analysis of the component scores. PCA is an analytical technique used in numerous studies of the spatial and temporal modes of atmospheric variability (Richman, 1986). It has also been used, with reasonable success, to carry out a simple comparison of observed Arctic sea level pressure patterns and GCM simulations (Crane and Barry, 1988). Volmer et al. (1984) also used Empirical Orthogonal Functions (EOFs) to examine the 500 mb patterns of the European Center for Medium Range Forecasting (ECMWF) model. In the present case, the principal components are extracted from the correlation matrix, and an orthogonal rotation is employed to enhance the interpretability and to avoid the creation of Buell patterns (Buell, 1979). Buell (1979) demonstrated that unrotated components have a tendancy to show a characteristic sequence ofpatterns; the first component being a weak center covering the whole spatial domain. The second and third components then tend to be bi-polar and orientated roughly 90^{o} to each other, while component 4 typically has four centers of alternating sign. This characteristic sequence of patterns makes it difficult to interpret the components in a spatial context, and Richman (1986) demonstrates that their spatial pattern has little meaning unless the components are rotated first. With rotation, the component axes are rotated such that the variable loadings on each component (i.e. the correlations between each component and the original variables) are maximized. In this case, each component tends to show a single center located in a different part of the spatial domain, which facilitates their interpretation in terms of regions of homgeneous variance. An orthogonal rotation is employed in the present study so that each of the rotated components still explains a

TABLE 1. PCA Results of the First Ten Eigenvalues of the NMC and GISS Data Sets

EIGENVALUES OF THE NMC CORRELATION MATRIX
TOTAL = 126
RETAINED = 7

	1	2	3	4	5	6	7	8	9	10
Eigenvalue	28.82	24.38	17.9	12.33	8.44	6.77	6.31	3.48	2.83	2.20
Explained Variance										
Proportion	0.22	0.19	0.13	0.09	0.06	0.05	0.05	0.02	0.02	0.01
Cumulative	0.22	0.42	0.55	0.65	0.72	0.77	0.82	0.85	0.87	0.89

PERCENT VARIANCE EXPLAINED BY EACH RETAINED ROTATED PC

PC Number	1	2	3	4	5	6	7
Variance	14.9	14.2	11.8	11.6	10.8	10.3	9.1

TOTAL = 82.7%

EIGENVALUES OF THE GISS CORRELATION MATRIX
TOTAL = 126
RETAINED = 7

	1	2	3	4	5	6	7	8	9	10
Eigenvalue	28.20	17.22	15.12	12.49	8.40	7.28	5.64	3.63	3.13	2.70
Explained Variance										
Proportion	0.22	0.13	0.12	0.09	0.06	0.05	0.04	0.02	0.02	0.02
Cumulative	0.22	0.36	0.48	0.57	0.64	0.70	0.74	0.77	0.80	0.82

PERCENT VARIANCE EXPLAINED BY EACH RETAINED ROTATED PC

PC Number	1	2	3	4	5	6	7
Variance	14.5	11.6	11.6	9.8	9.4	9.1	8.9

TOTAL = 74.9

unique portion of the original data set variance, It is also possible to carry out an oblique rotation, in which case there would be some correlation between components, and the variance explained by each component would no longer be unique.

Seven components were retained for rotation, with these components explaining 82% of the variance in the NMC data and 74% in the GISS (Table 1). There are several rule-of-thumb methods for deciding the number of components to retain, which in the present case was decided using a scree test. For both the NMC and the GCM analyses, however, the retained components also satisfied the Overland and Preisendorfer N test (Overland and Preisendorfer, 1982), indicating that it was reasonable to accept all seven components. Furthermore, the sampling error of the 7th eigenvalue was, in both cases, considerably less than the spacing between component 7 and component 8, indicating that the cut-off point did not fall within an "effective multiplet" created by sampling problems (North et al., 1982).

The component loadings for each grid point, which explain how each grid point loads on or is related to the component, are plotted as contour maps to provide a spatial representation of each component. These are interpreted as regions of cohesive spatial variance and, as such, they represent the principal modes of spatial variability in the data set. The temporal pattern of component change is determined using the component scores derived from the estimated score coefficients generated by the SAS PCA procedure (SAS, 1985). The time series of the component scores for each day show each component's contribution to any given days synoptic pattern. It is important to note, however, that PCA represents a linear filter and, while non-linear processes will have their linear relationships revealed by PCA, the linear correlations will underestimate the true value of the non-linear processes. The component patterns are, therefore, better thought of as the spatial representation of the primary modes of linear variance in the data set.

3. *THE SYNOPTIC-SCALE CIRCULATION*

Comparison of Spatial Patterns:

The representativeness of the model circulation is determined by correlating the observed and the modeled component patterns. Pairwise correlations of all combinations of the observed and the model components are calculated using Pearson's correlation coefficient to determine which, if any, of the NMC components are present in the model simulations. Richman (1986) suggests the use of a congruency coefficient for comparing component patterns as Pearsons's correlation removes the mean of each vector. In the present case, as we are comparing the results from the analyses of two different data sets, there is no reason to expect that their means should be the same. Furthermore, in this particular application we are interested only in how well the spatial patterns match, and Pearson's correlation provides an adequate measure for this purpose. Three sets of correlations are computed, one using the actual grid pointloadings and the other two using the north-south and east-west component loading gradients at each grid point. The measure of comparison, then, becomes the average of the three correlation coefficients. Such a procedure is necessary as the spatial positioning of centers of high and low values dominates the Pearson's correlation coefficient, which does not distinguish adequately the gradient or amplitude differences between grids. This may lead to anomalously high coefficients when only the grid point loadings are used.

The matching patterns in the two data sets are very distinct; for example, NMC component 1 correlates with GISS component 1 with an average r value of 0.94. The next best correlation for NMC component 1 is with GISS component 2, with an average r value of -0.51. Similarly, NMC

component 6 and GISS component 5 correlate with an average r value of 0.91, and the next highest correlation for component 6 is with GISS component 7, at -0.36, etc. (Table 2). In other words, there are no cases where

TABLE 2. Correlation Coefficients for all Pairs of NMC and GISS Components

NMC	GISS	Average	N-S Gradient	E-W Gradient	Grid-points
1	**1**	**0.94**	**0.97**	**0.91**	**0.93**
6	**5**	**0.91**	**0.97**	**0.84**	**0.92**
2	**3**	**0.91**	**0.95**	**0.85**	**0.92**
7	**4**	**0.91**	**0.97**	**0.87**	**0.87**
5	**7**	**0.90**	**0.96**	**0.87**	**0.86**
3	**2**	**0.89**	**0.96**	**0.81**	**0.91**
4	**6**	**0.87**	**0.94**	**0.75**	**0.90**
5	3	0.37	0.16	0.57	0.37
1	4	0.23	0.09	0.10	0.51
4	2	0.16	0.02	0.10	0.35
6	1	0.11	0.15	0.12	0.06
7	1	0.08	0.02	-0.20	0.41
3	7	0.06	0.31	-0.45	0.32
1	5	0.02	0.10	-0.01	-0.03
2	1	0.01	0.10	0.04	-0.11
3	6	0.00	-0.01	-0.19	0.19
4	7	-0.01	-0.18	-0.30	0.43
1	3	-0.02	0.00	0.12	-0.18
2	5	-0.03	0.07	-0.53	0.39
3	4	-0.04	-0.26	0.22	-0.07
2	7	-0.04	-0.19	0.21	-0.13
7	2	-0.05	-0.22	0.12	-0.05
7	3	-0.08	-0.36	0.17	-0.05
2	4	-0.11	-0.44	0.16	-0.05
5	2	-0.11	0.15	-0.62	0.12

Figures in bold are those correlations for which the average r was greater than 0.87 (75% of the variance in common)

TABLE 2. Correlation Coefficients for all Pairs of NMC and GISS Components

NMC	GISS	Average	N-S Gradient	E-W Gradient	Grid-points
4	1	-0.12	0.04	0.07	-0.48
4	5	-0.12	-0.40	0.36	-0.33
4	4	-0.13	0.07	-0.09	-0.35
6	6	-0.14	-0.42	0.33	-0.33
5	6	-0.15	-0.24	-0.43	0.22
6	3	-0.15	-0.01	-0.53	0.09
6	4	-0.15	0.05	-0.28	-0.23
7	5	-0.17	0.04	-0.28	-0.29
5	1	-0.18	-0.51	0.41	-0.45
5	4	-0.21	-0.33	-0.11	-0.20
3	3	-0.22	-0.08	-0.10	-0.49
1	7	-0.22	-0.51	0.28	-0.44
7	7	-0.23	-0.30	-0.23	-0.15
5	5	-0.25	-0.10	-0.20	-0.46
6	2	-0.26	-0.44	-0.06	-0.28
1	6	-0.26	-0.14	-0.13	-0.53
2	6	-0.33	-0.29	-0.48	-0.23
2	2	-0.34	-0.10	-0.41	-0.53
7	6	-0.35	-0.18	-0.36	-0.50
6	7	-0.36	-0.24	-0.14	-0.69
4	3	-0.39	-0.39	-0.64	-0.15
3	5	-0.39	-0.46	-0.29	-0.43
3	1	-0.43	-0.54	-0.35	-0.38
1	2	-0.51	-0.58	-0.50	-0.45

Figures in bold are those correlations for which the average r was greater than 0.87 (75% of the variance in common)

a component in one set has a high correlation with more than a single component in the other. It is also interesting to note that the first three components have an almost one to one correspondence between the two

sets (eg. NMC 1 matches GISS 1, 2 matches 3, and 3 matches 2) indicating that not only do the patterns match, but they have similar ranks in their contribution to each data set's total variance. The matching components in the two sets also have similar levels of explained variance (Table 1), although the GISS components tend to explain slightly less of the variance than do the corresponding NMC components. The GCM in this case may have less coherence in its spatial representation of the circulation patterns due to the simplifications and parameterizations involved in the computations. This would lead to the variance being slightly less concentrated in the principal eigenvectors. Figure 2 shows the loading patterns for each pair of GISS and NMC components. Remembering that PCA picks out the primary modes of variance, then what the loading pattern indicates is a region of similar variance in the data set. The region of high loadings in Component 1, for example, extend over about 2000 km centered on southern New Mexico. This pattern, which is the dominant mode on the synoptic time scale, may be indicative of cut-off low regeneration or a southern storm-track. However, it should be remembered that these components can not be directly interpreted in terms of characteristic synoptic "types". The actual circulation on any particular day will be made up of some weighted combination of all of the components, and the components themselves simply represent patterns of regional variance, with centers that are roughly synoptic-scale in extent. Bearing this in mind, however, it is still possible to suggest some physical interpretation for the location of each of the patterns in terms of the synoptic features that would contribute most to patterns of variance depicted by each component. Component 2 could be thought of as representing systems moving from the Gulf Coast and along the Mississippi and Ohio Valleys, Component 3 primarily reflects the strengthening and weakening of the Bermuda High, and Component 6 represents the contribution to the variance due to intrusions of the Canadian continental high pressure system.

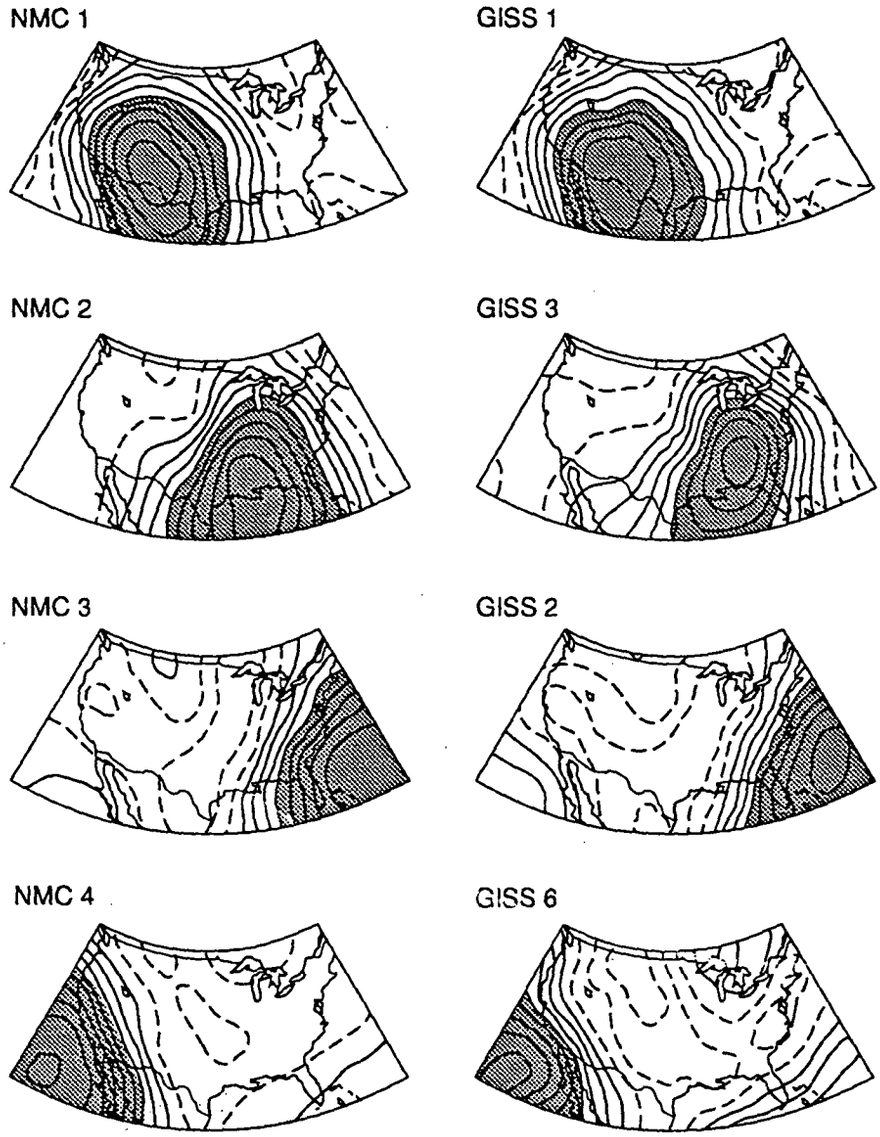

Figure 2 **Matching Pairs of NMC and GISS Component Patterns**

The contributions to components 4 and 7 would be due primarily to Pacific systems entering the south-west and north-west respectively, while Component 5 would reflect systems moving out to the north-east.

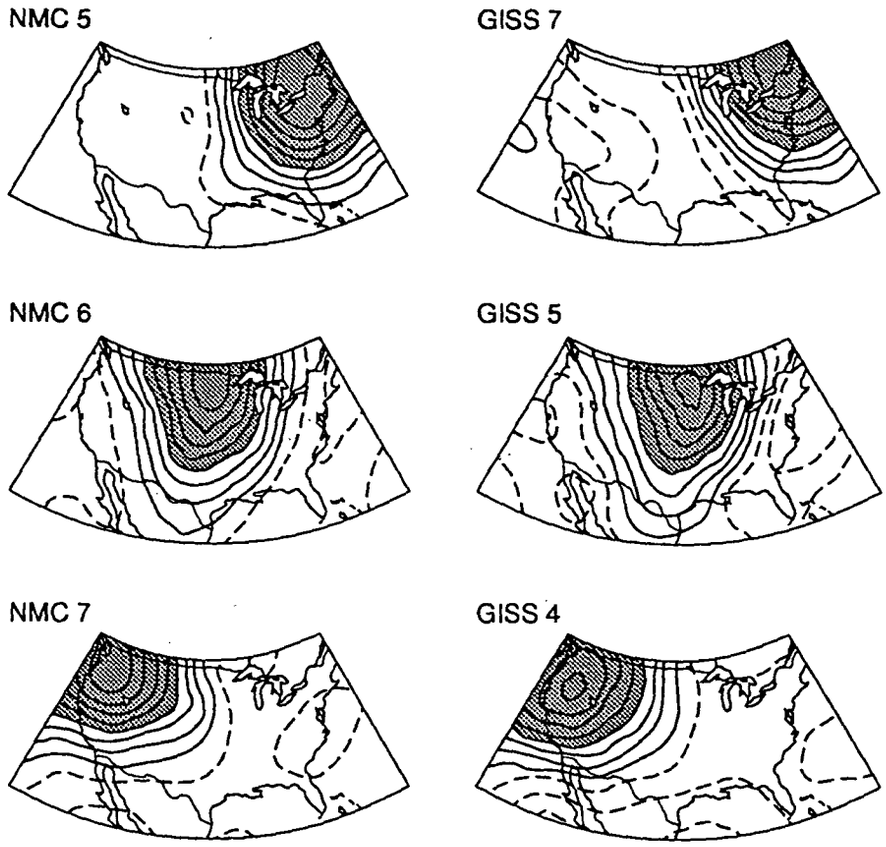

Figure 2. **Continued**

Temporal Correlations:

The correlation of the component loadings points to good agreement between the model and the NMC data in terms of their spatial patterns and their contibution to the variance of each data set; that is, both show the same synoptic-scale atmospheric circulation features. The next test is to determine whether these synoptic-scale features have similar temporal characteristics. The explained variance of each component shows how important it is to the overall variance in the data set, but it does not reveal

how the component behaves with time (i.e., the frequency of observation or reoccurrence). The temporal patterns are, therefore, examined using Fourier analysis of the component scores to show the dominant periods in their temporal occurrence. The power spectra of those components that have similar spatial patterns are correlated to determine whether they have similar spectral peaks. Since the component score time-series of the NMC and GISS data sets are of different durations, a spectral decomposition results in power estimates for the two sets which have a different number of frequencies spaced at differing intervals. To overcome this, the individual spectra are binned at half-day intervals, and pairs of spectra are correlated using Pearson's correlation coefficient over three band widths from 2-12 days, 10-31 days, and 2-31 days. All of the binned spectral series are given a minimal smoothing with a three-day moving average filter having weights of 0.5, 1.0, and 0.5. As the coefficients only demonstrate how well two variables co-vary, the series are integrated to obtain the total power for each bandwidth, and the totals are ratioed to give an index of how much power was contained in the NMC data with respect to the GISS data. The power ratio is calculated using:

$$Pr = 1 - NMC / GISS \text{ for NMC total power} > \text{GISS total power} \quad \text{(EQ 1)}$$

or

$$Pr = -(1 - GISS / NMC) \text{ for GISS total power} > \text{NMC total power} \quad \text{(EQ 2)}$$

This results in the larger power always forming the denominator, and the result is made negative if the denominator is the NMC value. The power ratio, therefore, varies from +1 to -1 with zero indicating that the powers match, and the sign indicating which data set contains more power within a given frequency band.

The temporal correlations were not quite as satisfactory as those obtained for the spatial analysis (Table 3), with the components that had high spatial correlations only having similar spectral peaks in the 2-12 day

period. Table 3 does serve to indicate, however, that the model is at least

TABLE 3. Temporal Correlations and Power Ratios for all Component Patterns Having a High Spatial Correlation

Components		2 to 31 days NMC/GISS		2 to 12 days NMC/GISS		10 to 31 days NMC/GISS	
NMC	GISS	r	ratio	r	ratio	r	ratio
1	1	0.26	-0.28	0.80	-0.11	0.12	-0.35
6	5	0.10	-0.43	0.66	-0.35	0.60	-0.16
2	3	0.49	-0.04	0.77	-0.28	0.45	0.17
7	4	0.36	-0.16	0.60	0.22	0.30	-0.07
5	7	0.28	-0.18	0.80	0.05	0.57	0.11
3	2	0.11	0.05	0.20	0.27	0.25	0.03
4	6	-0.12	0.31	0.88	0.23	0.62	0.49

See text for an explanation of the NMC/GISS power ratio

determining the broader, more fundamental, synoptic features with reasonable temporal accuracy. The high correlation between NMC component 1 and GISS component 1 in the 2-12 day bandwidth suggests that the sequence of pressure changes that occur with the passage of cyclones through the region takes the same amount of time in the model as it does in reality. The same is true for the other pairs of NMC and GISS components that appear to be influenced by cyclonic systems moving through the region. Similarly, for NMC component 6 and GISS component 5, the high correlations at 2-12 days shows that the advance and retreat of the semi-permanent Canadian high pressure system correlates well with the model's high pressure system in the short time frame, and the same can be said for the Bermuda High (NMC 3 and GISS 2). In other words, the model correctly determines the rate of advance and retreat of these highs, or the development or movement of low pressure systems. That the correlations are generally poor at the longer time scales simply indicates that the pressure system repetition, or timing of events, is different between the model and the NMC data. For most cases there is, however, near

equivalence in the total power contained in the 2-31 day bandwidth showing that these features still explain similar amounts of variance in the model and the observed data on the monthly time-scale.

4. REGIONAL CLIMATE CHANGE ASSESSMENT

The Earth is a complex system defined by an intricate set of interactions and exchanges between system components. These interactions involve all aspects of the physical and human environment, and occur over a wide range of time and space scales. In terms of its ability to support life, this system has remained remarkably stable over several billion years; however, within these broad limits the Earth has undergone considerable change over time. Although change within limits is an integral feature of the Earth System, as we move into the 21st century a major scientific question arises with regard to the present rate of change, and the degree to which it is human-induced.

Humans impact the system in a variety of ways, with the greatest concern being the potential for global-scale warming that may accompany anthropogenic increases in atmospheric greenhouse gases. Much of the research in this area is driven by the recognition that we have only a limited understanding of the climatic consequences of these greenhouse gas increases, and by the further recognition that such potential climate change could have a severe impact on human systems. Consequently, the goal of the U.S. Global Change Research Program is, "to establish the scientific basis for national and international policy making related to natural and human-induced changes in the Global Earth System" (Committee on Earth Sciences, 1989). Their motivation for this is dictated by the need to predict potential change with sufficient accuracy to allow for the timely formulation of planning and policy-making decisions. However, the potential for rapid change places a severe constraint on our abil-

ity to make such predictions in time for effective planning to occur. This time limitation is compounded by the fact that all such planning has to be regional in nature, and by the long lead time necessary to instigate societal and economic modifications in human systems.

Approaches to climate change prediction can follow several different lines:

- the prediction may be conceptual in nature, based on our present understanding of how physical and human systems operate;
- they may be derived by analogy with past climates; or
- the climate change may be simulated through the use of numerical models of system processes.

Of these, the first approach is limited by its inability to provide quantitative predictions for specific regions. The second method can derive such predictions; however, as the forcing functions are different, there is no way of ensuring that warm climates in the past are analogous to those that may occur in the future (c.f. Mitchell, 1990; Crowley, 1990). As numerical process models have the potential to overcome both these limitations, then General Circulation Models (GCMs) of the atmosphere and oceans are the most frequently used tools for global change prediction.

Unfortunately, GCMs are also beset with problems--the most notable of which are the inadequate treatment of some of the physical processes, and the relatively coarse spatial resolution of the model simulations. As a consequence, the models appear to do an adequate job of reproducing the large-scale climate, but there are large uncertainties in their simulations of individual grid-point values. Similarly, while most models agree on the extent of CO_2 warming at the global scale, inter-model comparisons show large differences in the regional expression of this change (Schlesinger and Mitchell, 1987; Grotch et al., 1991). While many scientists will accept the idea of a general warming due to increased CO_2,

there is a much greater uncertainty with regard to the magnitude of the warming, and very little confidence in the ability of the GCMs to accurately predict individual grid-point temperature changes.

While research in GCM development continues, several possibilities exist for regional scale analyses utilizing the current model capabilities. The first is simply to use the model predictions of grid-point climate variables, and work along these lines has been conducted by Becker and Nemec (1987). Given the large uncertainties in the grid-point climate predictions, however, this does not appear to be a particularly useful way to go. Furthermore, this method is still limited by the grid-point resolution. The question of resolution limitations has been addressed by Wigley et al. (1990) and Karl et al. (1990) who estimate the regional or local scale temperature and precipitation from the GCM grid-point climate data. This provides an estimate of the local climate, but it is still limited by the accuracy of the GCM climate change predictions. A second possibility is to use mesoscale climate models. These models have met with considerable success when driven by observed climate fields, and the possibility arises for driving these models for specific regions, using the GCM fields to set the boundary conditions. Giorgi (1990), for example, has driven the Pennsylvania State University/NCAR mesoscale model (MM4 at 60 km resolution) for the western United States, using two different versions of the NCAR Community Climate Model (CCM). The nested approach improved the temperature and precipitation distributions, and it is apparent from the simulations that mesoscale models have the potential to produce the data needed for regional scale analyses. For climate change predictions, however, mesoscale models still suffer from the fact that the boundary conditions are set from GCM fields in which we can have very little confidence. A third approach, and the one that is used here, is to take a feature of the GCM in which we do have a large degree of confidence (in this case the synoptic sea level pressure distribution), derive transfer functions between this feature and the grid-point temperature distribution using observational data, and use the change in

synoptic circulation in the doubled-CO_2 climate to predict future changes in temperature. The objectives here are to examine the performance of the GCM at the grid-point scale, to determine whether the model is adequately reproducing the short-term (synoptic-scale) variability that is averaged to produce the monthly means normally presented in GCM analyses, and to explore the possibility that observed relationships between sea level pressure and the surface air temperature may provide a means for determining how the large-scale temperature change predicted for a doubling of atmospheric CO_2 may be distributed at the grid-point or regional level.

The methodology arises from the premise that daily temperature distributions in the extra-tropics are largely a function of the synoptic-scale circulation. In other words, while seasonal anomalies may be set-up by larger scale processes (e.g. anomalous sea surface temperatures), the local distribution of these effects are felt through changes in the circulation; large-scale processes determine the position and intensity of the jet stream, for example, which sets up a preferred circulation regime, which then impacts on local climate. In this paper, therefore, we focus on the relationships between the synoptic-scale circulation and the local temperature. We use these relationships to examine the synoptic-scale performance of the GCM, and to show how the changes in synoptic circulation in a doubled CO_2 climate may affect the regional distribution of the predicted large-scale warming. For climate change predictions, the technique rests on several hypotheses that we can test, and several assumptions that we have to accept, but which add some uncertainty to the results. For this technique to work, it is necessary that:

1) the models accurately simulate the present synoptic-scale atmospheric circulation;

2) that accurate transfer functions can be derived to estimate regional temperatures from the circulation characteristics; and

3) that in a doubled CO_2 world, the underlying modes of the circulation will remain the same, and that only the frequency, persistance, and intensity of individual events may change.

The first requirement was examined in Section 3, and the analysis showed that the model effectively reproduces the observed circulation fields. In Section 5 we show that accurate temperature transfer functions can be derived for most of the United States. The third hypothesis is tested in Section 6 and is also found to be valid. The transfer functions are then applied to a doubled CO_2 run of the same high resolution GISS model, and the results show very different distributions of North American temperature change than have previously been obtained for a doubled CO_2 climate. As noted above, these regional predictions are based on a variety of assumptions concerning the behavior of the climate system in a doubled CO_2 mode, and these are discussed further in Section 6 below.

5. SYNOPTIC CONTROLS ON TEMPERATURE

The second hypothesis--that the temperature distribution is largely a function of the synoptic-circulation--is tested by deriving transfer functions between the circulation modes and grid-point temperatures(using the observed data), and by comparing the observed fields with those predicted by the transfer function for an independent test data set. The temperature transfer functions are derived for January and July, and the principal components analysis has been repeated for these two months individually. The principal components analysis of the individual months produces similar results to those described above and, again, seven components are retained for each data set in both months. In this case, the analysis is carried out for 19 years of January and July data from 1966 to 1973, and from 1977 to 1987. The three years from 1974-

1976 are retained as a test data set to validate the transfer function predictions. Again the data are from 1200z, and thus represent early morning temperatures over the U.S.

The transfer function takes the form of a stepwise polynomial regression model, with a separate model being derived for each season and for each individual grid-point. The dependent variable for each model is the grid-point temperature from the NMC grid; the independent variables used in the model are the component scores from the principal components analysis of the observed circulation fields. Each model uses a set of lagged component scores consisting of the seven scores for the day in question, as well as the scores from the previous two days. The scores represent the contribution of each circulation mode to the pressure pattern for that day, and the lagged scores account for the evolution of the systems through time. The regression coefficients derived from the lagged component scores account for the direct effects of air mass source region and its modification through transport--a strong low pressure system to the north-east, for example, which brings cold air from the north. The secondary controls on temperature, such as cloud cover and precipitation, are captured by the cross-products of the circulation component scores in the regression model. The cross-products represent the interactions between components such as, for example, the cross product between the score on component 6 (the Canadian High) and the previous day's score on component 3 (the Bermuda High), which gives some indication of how the synoptic characteristics of the warm moist air from the Atlantic are modified by the advance of cold Arctic air from the north.

The lagged scores, their squares, and their cross-products result in 252 possible variables from which the regression model can draw. Each variable is evaluated for its individual significance level, and the variable is entered in a stepwise manner if it is significant at the 85% confidence level. The variables in the model are then re-evaluated at each step, and

only those variables are retained who's contribution to the model is significant at the 99% level. The daily component scores for the 19 years result in 589 observations, and the regression equations for each grid-point in each season are found to contain between 7 and 26 of the possible 252 variables.

Once generated, the transfer functions are applied to the days in the three-year test data set, and the derived grid-point temperature values are compared to those contained in the NMC grid-point data set. The results are presented in Figure 3, which shows the correlation between the observed and the predicted temperatures at each grid-point. As would be

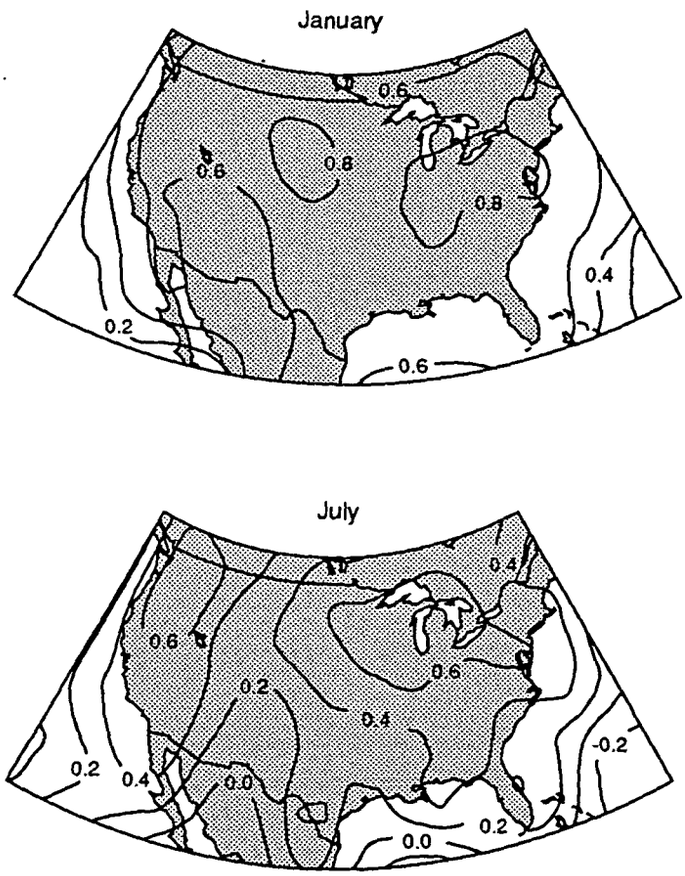

Figure 3. **Correlations between observed temperatures, and temperatures predicted by the temperature transfer functions**

expected, the January correlations are high over most of the country, while the area of high correlation is somewhat reduced in July. The low correlations found over much of the south, Florida, and the western Great Plains in July are probably due to the stronger influence of convective processes during the summer season. The shaded regions are those areas having correlations greater than 0.5 in January and greater than 0.4 in July. Statistically, an r value of 0.35 is significant at the 0.1% probability level; however, it appears from a simple visual analysis of the predicted and observed temperature time-series for grid points with differing correlation coefficients, that correlations of at least 0.5 and 0.4 are necessary for generating justifiable monthly means. An examination of these time-series also shows that the temperatures predicted by the temperature transfer function match the phase and the amplitude of the grid-point temperature records, with the exception of the extreme event amplitudes (which are normally not captured by a regression model). Even more impressive is the fact that the transfer function can match day-to-day temperature swings in excess of 20°C in January.

Table 4 compares the performance of the monthly mean fields derived from the temperature transfer functions with the observational data and the GCM simulations of present-day January temperatures. The table shows the correlations and root mean square error (RMSE) for the grid-point values and the north-south and east-west gradients, for various different fields. The first row compares the transfer function predictions with the observational data for the three year test period, and row two compares the transfer function predictions for the test period with the 21-year observational mean. It is interesting to note that both the correlations and the error improve slightly when compared with the long-term mean, which is simply indicative of the variability present in the three year test period. Row three compares the 21-year observational mean with the 3-year mean from the GCM simulation of the present-day climate; the correlations are good, but are lower than those obtained with

the transfer functions. Row three shows that the model obtains the cor-

TABLE 4. Comparison of the Temperature Transfer Function Results with the NMC Data and the Present-Day GCM Simulations (January)

	Grid-points		N-S gradients		E-W gradients		Average	
	r	rms	r	rms	r	rms	r	rms
Observed v Transfer Function (3 year test period)	0.99	1.71	0.94	0.91	0.98	0.84	0.97	1.15
Transfer Function (3 year) v 21 Year Observed Mean	0.99	0.44	0.97	0.39	0.99	0.34	0.98	0.39
21 Year Observed Mean v 3 Year GCM Mean	0.97	2.33	0.81	1.06	0.92	1.96	0.90	1.79
21 Year Observed Mean v Transfer Functions on GCM Circulation	0.98	1.41	0.93	0.80	0.96	0.89	0.95	1.03

r is the average correlation at all grid-points

rms is the root mean square error averaged over all grid-points

rect pattern of temperature distributions (i.e. high correlations on the grid-point temperatures), but that the gradients are less well matched (particularly the north-south gradients). This supports the general observation that the GCM can simulate the larger scale cirulation field very accurately, while being much less reliable at predicting local (grid-point) temperature distributions. Similar results were obtained by Walsh and Crane (1991) who showed that, in a comparison of five different GCMs, the model that produced the most accurate sea level pressure field over the Arctic also had the least accurate temperature field. The last row of Table 1 compares the 21-year observed mean with the temperature distribution derived by applying the transfer functions (from the observed data) to the circulation from the GISS model. In each case, this results in

higher correlations and lower errors than those obtained when comparing the model derived temperatures to the long-term mean; the average correlations increase from 0.9 to 0.95 (a 10% increase in explained variance) and the average RMSE drops from 1.79 to 1.03 (a 42% decrease). The improvement is even greater in the gradient comparisons, where the north-south gradient correlations increase from 0.81 to 0.93 (a 21% difference in explained variance).

A better idea of the extent of these differences can be seen in Figure 4, which shows the observed mean January temperature field (4a), and the present day temperatures simulated by the GISS $4^{o}x5^{o}$ GCM (4b), and the temperatures derived by applying the temperature transfer function to the GISS synoptic circulation (4c). In each case, these are presented as departures from the map means, and the regions masked out in Figures 4c, 4d, and 4e are those grid points for which the correlation between the original NMC test predictions and observations did not match the 0.5 correlation threshold. Comparing figures 4b and 4c with 4a we find that all three show the same general pattern of north-south temperature gradients (hence the high correlations in Table 4), but with a much reduced temperature gradient over most of the country in the GISS simulation. The GISS simulation, on the other hand, has much steeper temperature gradients over the oceans (along the coastline), and has much higher temperatures in the East and lower temperatures over the West.. As was shown in Table 4, however, the temperatures predicted by the temperature transfer functions reveal a much closer match to the long-term mean, and Figure 4c shows that the transfer functions produce gradients that are more realistic. In this case, the East is cooler and the West much warmer, and the moderating effects of the marine influence on coastal temperatures is much more apparent.

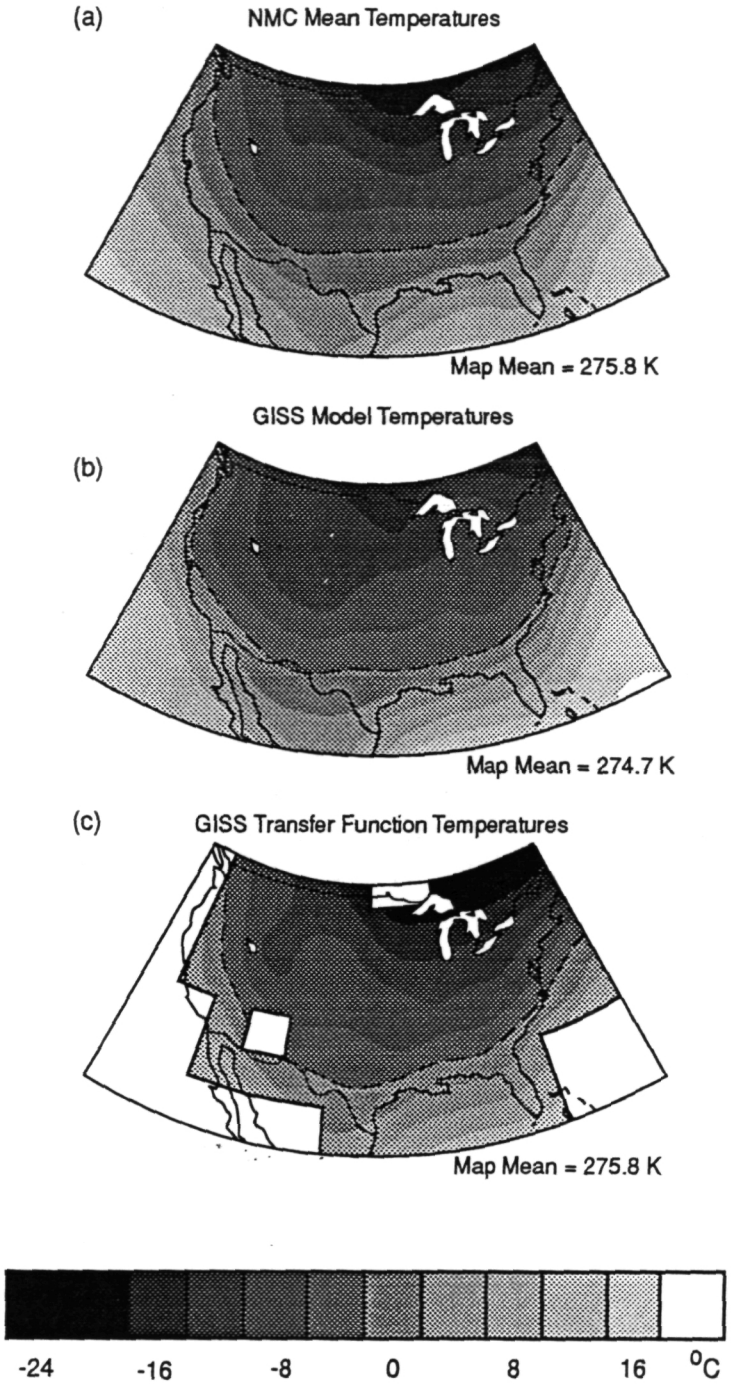

Figure 4. **Mean January temperatures: (a) observed, (b) GISS simulation, (c) transfer functions applied to the GISS circulation**

While the transfer function temperatures provide a much better fit to the observed long-term mean than do the model temperatures themselves, we should not expect an exact match in either case. As there is some interannual variability within the model, and the model climate is derived from only three years of data, it is possible that these three years could be different to the long-term mean. If the model is an accurate representation of the climate system, however, it should also demonstrate the same relationships between temperature and the atmospheric circulation that are present in the observed data. In which case, the temperatures predicted by applying the transfer functions to the GCM circulation should match reasonably closely the actual temperatures simulated by the GCM itself. Rather than comparing the GCM temperaturesto the observed mean, therefore, a more valid assessment of the model's ability to simulate the present day temperature field is given by comparing Figure 4b and 4c. In other words, the temperatures predicted from the model's actual circulation are a better indication of what the temperature field should be, than are the temperatures from the observed long-term mean. This comparison is shown in Figure 5a as the difference between the two fields (4c minus 4b). The figure reveals some obvious spatial biases in the GISS temperature simulation, with the north-east being up to 10°C too warm, and the west coast being 6°C - 7°C too cool. For comparison, the spatial bias in the transfer functions is given by Figure 5b, which shows the difference between the observed data and the temperatures predicted by the transfer functions for the three year test data set. The figure shows that the transfer functions are able to predict the mean January temperature to within +/- 1.5°C over most of the study area, but with a tendency for over-prediction in the north-west and south-east, and some under-prediction in the south-west and north-east.

In July, the GCM simulations result in a poorer match to the long-term mean, particularly in the gradient correlations, and the performance of the transfer functions is also considerably reduced. In this case, onlyabout

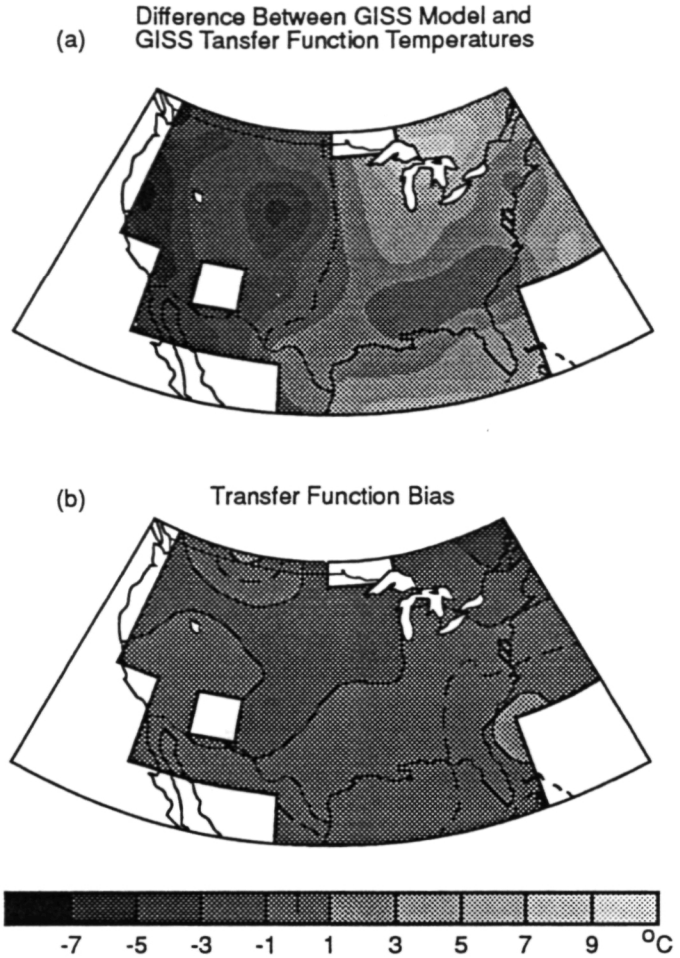

Figure 5. **Spatial Bias in the GISS simulated temperatures and in the temperature transfer functions (January)**

half of the study area satisfies the test criteria for the transfer functions, and the results presented in Table 5 are limited to these areas. Overall, the

TABLE 5. Comparison of the Temperature Transfer Function Results with the NMC Data and the Present-Day GCM Simulations (July)

	Grid-points		N-S gradients		E-W gradients		Average	
	r	rms	r	rms	r	rms	r	rms
Observed v Transfer Function (3 year test period)	0.98	1.30	0.71	0.77	0.77	0.65	0.82	0.91
Transfer Function (3 year) v 21 Year Observed Mean	0.99	0.27	0.96	0.30	0.99	0.21	0.98	0.26
21 Year Observed Mean v 3 Year GCM Mean	0.92	3.00	0.37	1.46	0.21	2.11	0.50	2.19
21 Year Observed Mean v Transfer Functions on GCM Circulation	0.73	2.15	0.39	1.75	0.54	1.87	0.55	1.92

r is the average correlation at all grid-points

rms is the root mean square error averaged over all grid-points

temperature distribution in the long-term NMC data is more closely matched by the temperature transfer functions than it is by the model, which, in this case, has steeper gradients over most of the country (Figure 6). Figure 7 shows the spatial bias in the GCM and in the temperature transfer functions, but, even taking these into account, it is evident from Figure 7a that there are again some marked spatial biases in GCM temperature simulations, with the model producing temperatures that are slightly too high over the Great Lakes, Florida, and the Gulf Coast, and temperatures that are too low over the west coast.

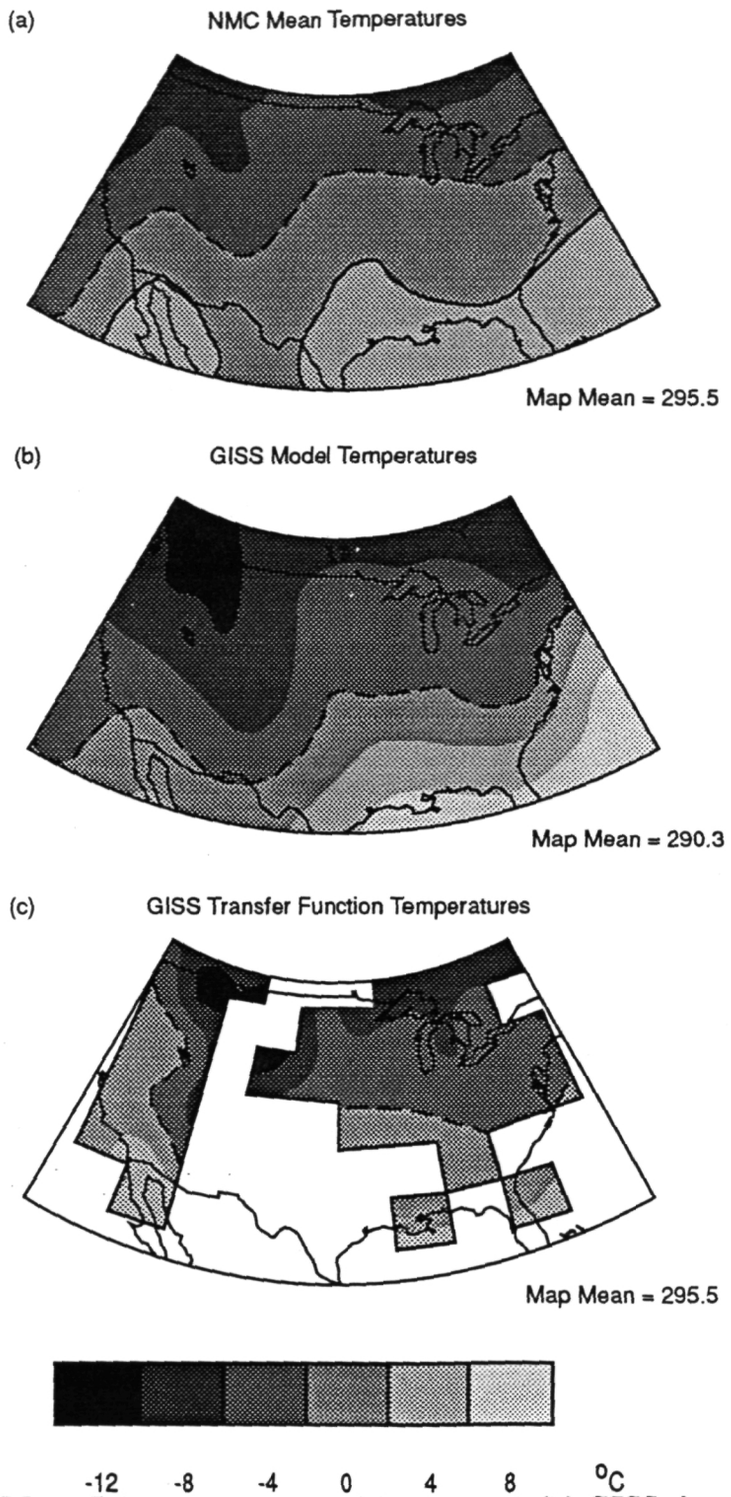

Figure 6. **Mean July temperatures: (a) observed, (b) GISS simulation, (c) transfer functions applied to the GISS circulation**

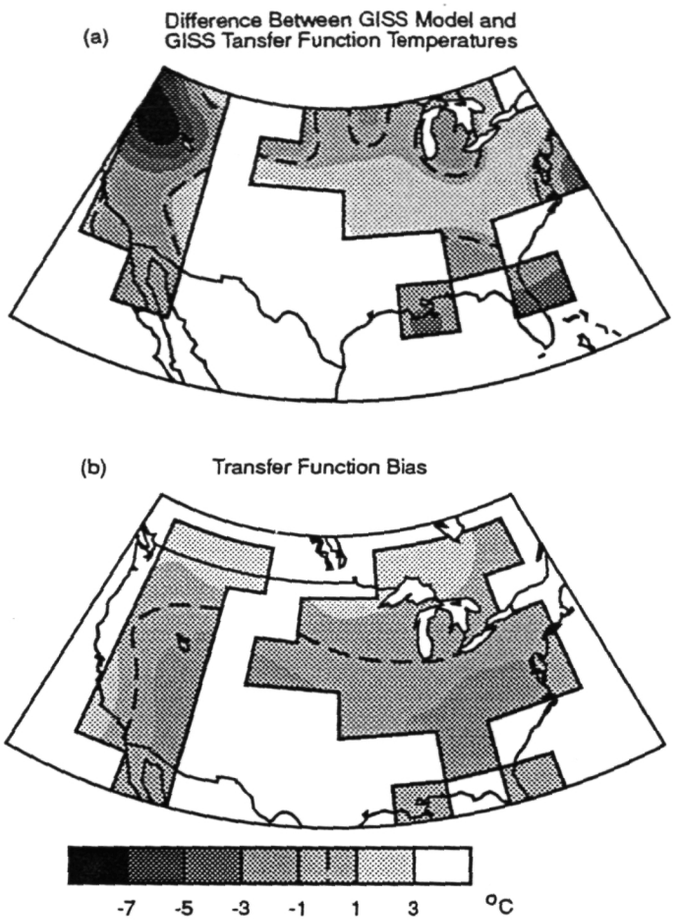

Figure 7. **Spatial Bias in the GISS simulated temperatures and in the temperature transfer functions (July)**

6.THE DOUBLED-CO2 CLIMATE

In order to assess the change in synoptic circulation that will occur with a doubling of atmospheric CO_2, the principal components analysis is applied to a $2xCO_2$ run of the same $4^o x5^o$ GISS model, and the results are compared to those obtained for the control run. The analysis was again-

carried out for January and July, and the same number of components were retained as before. The correlation analysis of the component loadings show that the same synoptic patterns are present in the doubled CO_2 climate. Again, there is a one-to-one match between the patterns; in this case, however, the match is not between components having similar rankings. In other words, the same circulation features are present, but they account for different amounts of the data set variance than they did in the GCM simulation of the present climate.

Describing the way in which the synoptic-scale circulation has changed is not straight forward. As the analysis does not identify discrete synoptic "types" we cannot simply count the change in frequency of occurrence, or the number of times one type follows another, etc. Consequently, the way in which the synoptic circulation has changed between the single and doubled CO_2 climates is examined through several Fourier-based indices. The indices are derived from the daily time series of component scores for both months, and for each year of data (3 years for both the $1xCO_2$ and $2xCO_2$ runs). For each sub-series (i.e. each month and year), the trends are removed from the component scores, and the sub-series variance and power spectra are calculated. The sub-series variance and power spectra are then averaged over the three years to produce mean January and July values. Following this:

1) the change in the total data set variance explained by the components gives some indication of the change in frequency of occurrence of the circulation modes. That is, the more frequently they occur, the greater will be their relative contribution to the data set variance. However, the variance may also change as the amplitude or intensity of the pattern changes, and a further calculation is necessary to separate out the amplitude change. In order to do this,

2) the total power of the average spectrum is calculated. The total power is simply the variance of the individual component time series, and

3) the power spectra and period series are standardized, and a least squares regression is fitted to the spectra. The gradient of this line is used as an index of power distribution versus period, and the change in gradient from the 1x to the 2x CO_2 climate--together with the change in power--then gives an indication of the change in synoptic characteristics.

A power change without a change in the gradient index reflects a change in intensity; if both change, and the change in power and the gradient index have the same sign, it represents a shift in the frequency of occurrence; and if the change is of opposite sign it reflects a change in persistance. The way in which this works is best shown by a diagram (Figure 8). Figure 8a is an example of a time-series of component scores showing a complex pattern of intensity, persistance, and frequency of occurrence. Figure 8b is an idealization of how the power spectrum for such a time-series may look, with a least squares regression line fitted. Figures 8c, 8d, and 8e represent ways this time series may change in a different climate. If the time period is held constant and the power spectrum remains the same (i.e. the slope of the regression line does not change), the variance can only change by increasing or decreasing the intensity (amplitude) of the signal (Figure 8c). If the variance increases but the gradient ratio also shifts to higher frequencies (i.e. the slope of the regression line increases), as long as the time period is constant, this can only happen if the number of peaks in the time-series (frequency of occurrence) increases (Figure 8d). Finally, if the variance increases but the shift in the index is to lower frequencies, this implies greater persistence (Figure 8e). By the same token, the opposite of these can also happen; if the index shifts to lower frequencies and the variance also decreases then the frequency of occurrence must have decreased, and if the variance decreases while the index increases, it would imply reduced persistance.

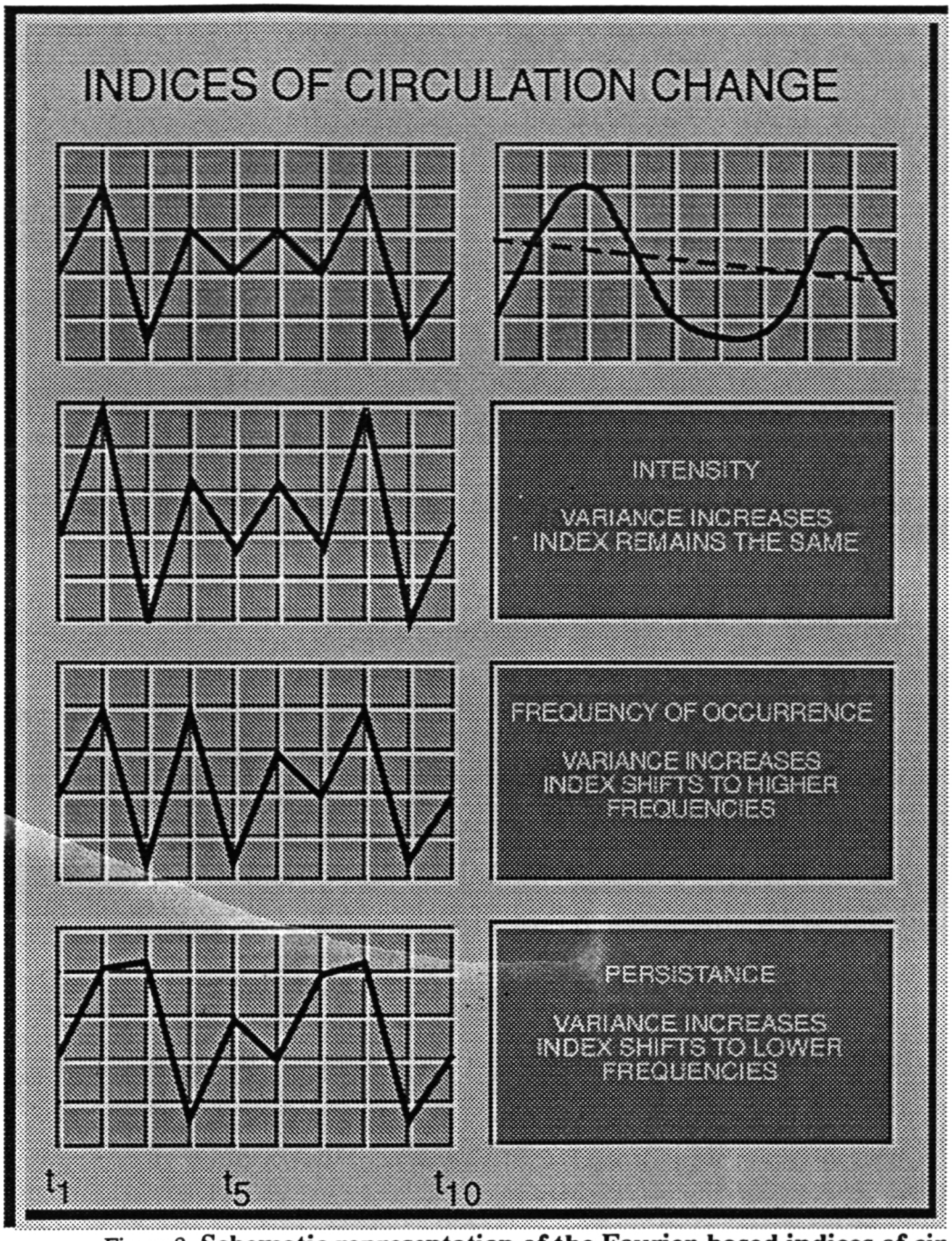

Figure 8. **Schematic representation of the Fourier-based indices of circulation change**

The results shown in Table 6 indicate several interesting changes: component 6 (the Canadian high pressure system) occurs as frequently as in the present-day model climate, but with reduced amplitude (intensity), while component 3 (the Bermudan High) maintains the same intensity but has a reduced frequency of occurrence. The frequency of systems

TABLE 6. Changes in Synoptic Circulation from a $1xCO_2$ to a $2xCO_2$ Climate

	Components						
January	**1**	**2**	**3**	**4**	**5**	**6**	**7**
1xCO2							
Power	2.03	1.06	1.25	1.39	0.87	2.03	1.00
Power Gradient Index	0.53	0.53	0.54	0.88	0.64	0.97	0.60
2xCO2							
Power	1.15	1.39	0.65	0.82	1.19	1.20	0.89
Power Gradient Index	0.74	0.76	0.65	0.61	0.67	0.91	0.80
July							
1xCO2							
Power	1.72	0.99	1.98	1.32	1.68	1.59	2.48
Power Gradient Index	0.80	0.88	0.43	0.78	0.82	0.70	0.35
2xCO2							
Power	0.95	0.71	1.70	1.05	0.94	0.96	1.77
Power Gradient Index	0.45	0.60	0.69	0.93	0.79	0.93	0.51

See text for an explanation of the Power Gradient Index

moving from the Pacific and into the north-west (component 7) decrease,

while those moving into the south-west have the same frequency, but lower persistance (which might imply that they are moving faster). Systems moving off the Gulf and into the central U.S. (component 2), on the other hand, show increased persistance. In the model's doubled CO_2 climate, it would appear that the semi-permanent high pressure systems have a reduced influence in the area, and that cyclone activity appears to be stronger in the south and weaker in the north. Again, it must be remembered that these changes apply to the modes of circulation ratherthan to discrete events. It would be possible for a day in the $2xCO_2$ climate to be dominated by an equal mix of components 2 and 6 (i.e. have high component scores on each), where the actual synoptic "change" would reflect the combined effect of the reduced intensity of the Canadian High and the increased persistance of low pressure systems in the Mississippi-Ohio river basins.

The effect of the circulation changes on temperature is shown in Figure 9, which presents the grid-point temperature change from the single to the doubled CO_2 climate, derived by applying the temperature transfer functions to the circulation data, which are then compared to the temperature change predicted by the model itself. The regions masked out in Figures 9b and 9d are again those grid points for which the correlation between the original NMC test predictions and observations did not match the 0.5 and 0.4 correlation thresholds discussed in the previous section. As with Figures 4-7, these maps are derived from the $1xCO_2$ and $2xCO_2$ temperature fields expressed as departures from the map means. In the case of the GCM temperature predictions the change in map means is given in the Figure; for the temperature transfer predictions, however, both the $1xCO_2$ and the $2xCO_2$ temperatures were derived as differences from the present map mean. Figures 9b and 9d, therefore, represent the temperature change from the present day that can be attributed to the change in the synoptic circulation of the atmosphere over the study region.

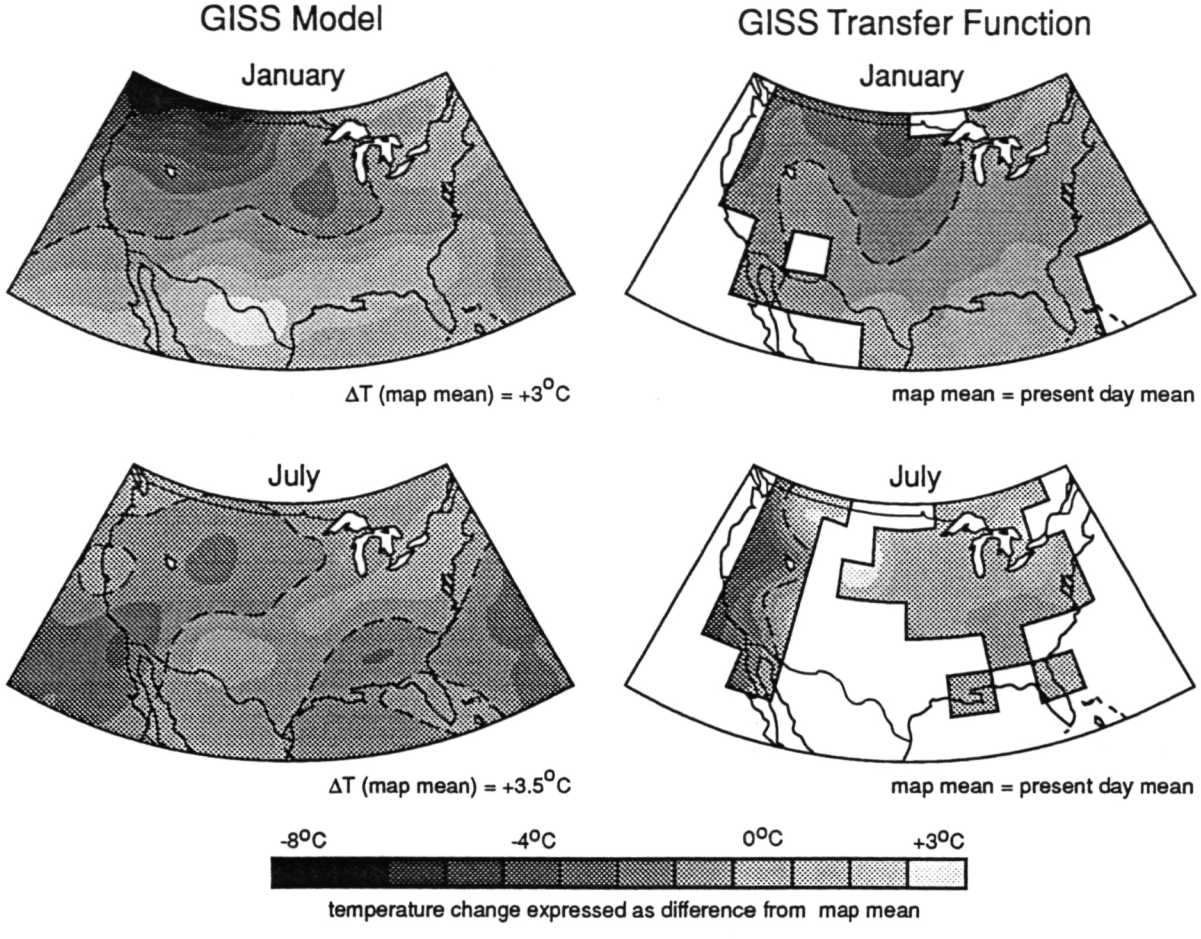

Figure 9. **2xCO2 temperature changes (difference from map means) predicted by the GISS GCM, and by applying the temperature transfer functions to the 2xCO2 GISS circulation**

It is important to recognize what is, and what is not, represented in these results. The transfer functions calculate the contribution to a grid-point's temperature that is due to the variability in synoptic-scale atmospheric circulation--the transfer functions do not account for changes that occur over larger temporal scales. Estimates of these larger scale changes,

however, can be obtained from the GCM climates. The temperature change in Figure 9 is presented in the form of differences from the map mean, which, for the GCM results, contain the changes due to time periods longer than the synoptic time-frame used here. The difference in map means between the $1xCO_2$ and the $2xCO_2$ GCM temperatures can, therefore, be added to the transfer function predictions in order to include an estimate of the larger scale changes.

A potentially more important problem is that the transfer function predictions show the changes that will occur due to a change in the circulation--assuming that the properties of the synoptic systems remain the same in a doubled CO_2 climate. If there is a differential change in source region temperatures; if sub-polar air masses, for example, show a greater or smaller degree of warming than sub-tropical air, this will result in a change in source region temperature that will not be reflected in the transfer function predictions. Similarly, if other properties of the air mass change (eg. the cloud cover or the cloud radiative properties), again this will not be included in the transfer function maps. The extent to which this is a significant problem is difficult to determine at present, but it is likely to vary from region-to-region. A typical winter low pressure system over the central U.S. is, in itself, not likely to have a very different cloud cover to the present, although the cloud amount in the region may change due to changes in the persistance of the systems, or their frequency of occurrence (in which case the change would be caught by the transfer functions). On the other hand, if there is a change in mid-latitude sea surface temperatures, then we could expect systems moving off the Pacific to be slightly warmer than present, and our west coast predictions may be low.

The effect of latitudinal differences in surface heating are more difficult to predict. Most GCM experiments show a high latitude enhancement of the surface air temperature increase, with the polar increases being 2x to 4x the mean global change. These results suggest a reduction in the

mean latitudinal temperature gradient, which again would imply differential changes in source region temperatures. GCMs, however, produce very poor simulations of the present day distribution of Arctic temperatures; they are unable to accurately simulate the present ice distribution; they have difficulty resolving the Arctic inversion; and they do a poor job of simulating Arctic clouds, all of which play a significant role in determining the surface temperature (Walsh and Crane, 1992). Ice-atmosphere processes are such that a high latitude enhancement of the global warming is very likely, but, given the difficulty that present GCMs have in simulating these processes, the magnitude of the effect is still questionable. Consequently, it is difficult to determine, at this time, whether or not there will indeed be a very large latitudinal difference that would have a significant impact on the transfer function predictions. Interestingly enough, however, the hypothesized reduction in north-south temperature gradients is shown by the January transfer function predictions to actually be greater than that predicted by the GCM itself. If we were to factor in increased source region temperatures in the north, the temperature gradient would be reduced still further, and would show an even greater difference to the temperature distribution predicted by the model.

Comparing 9a and 9c with 9b and 9d, even without factoring in the mean change, shows some interesting differences. While the GISS $4^{o}x5^{o}$ model shows a warming everywhere when averaged over the year, the January mean does in fact show a cooling in the north-west. Furthermore, the cooling occurs at all hours of the day, and is not simply a function of the early morning temperatures used here. This cooling is apparent in both the GCM and the temperature transfer function maps, but the temperature gradient is considerably higher in the GCM predictions. Overall, the GCM warms by about $3^{o}C$, but shows a relative cooling in the north-west and a warming in the south and east. When the map means are factored back in, this results in an absolute change of $-5^{o}C$ in south-west Canada, increasing to a $+6^{o}C$ change on the U.S.-Mexican

border. The transfer function, however, indicates a much weaker gradient, with the synoptic changes giving rise to a 2°C cooling in the north-central region and a 1°C warming in the north-east and along the Gulf coast (factoring in the change in map means from the GCM would result in a 1°C warming in the north and a 4°C warming in the south and east). Overall, the indication is that the January cooling in the north-west will be much less than is suggested by the GCM and, furthermore, while the large-scale patterns are consistent between the two, there is a major difference over the Rockies, which show a slight relative warming in the transfer function predictions that is not apparent in the GCM at all. In July the regional differences are even larger. The GCM warms by about 3.5°C overall, with relative changes between -2°C and +1°C. In this case, the transfer function predicts larger regional gradients with changes ranging from +3°C to -3°C, and with the greatest relative cooling over the west coast.

Despite some remaining uncertainty in the magnitude of the general warming that may occur with a doubling of atmospheric CO_2, we can make several observations on the possible temperature change in this area. For example, even if mean air mass characteristics change, the change in circulation indicated by the GISS model should promote relatively cooler temperatures in the north central region in winter, and on the west coast in both seasons (relative to the increases over the rest of the region).

Furthermore, it is very likely that some sort of temperature change having this relative spatial distribution will in fact occur. There is no doubt that the atmospheric concentration of CO_2 is increasing, or that this increase must have a direct radiative impact on the climate system. Calculations show that the direct radiative effect of doubling atmospheric CO_2 will be about a 4 Wm^{-2} warming--equivalent to a temperature increase of about 1°C. GCMs show that the feedbacks in the climate system will tend to amplify this warming. Debates then arise over the way

in which the potential feedback processes are treated within the GCMs. Due to the limitations in the current GCMs it is possible to argue that the feedbacks may not be as strong as the models suggest; that the positive feedbacks may, in fact, be greater; or, from the more extreme viewpoint, that the net effect will be a negative feedback and an overall warming will not occur.

These debates tend to obscure the fact that, regardless of the magnitude of the feedback processes, some climate change has to occur. Even if the net effect results in a global mean surface temperature the same as today's, in order to adjust for the increased radiative input we must achieve that temperature with a climate different to today's. Taking the less extreme view, all of the models indicate that the net feedback is positive. As the models do a reasonable job of simulating the broad-scale features of the climate system, there is a good possibility that there will be a tendency towards the types of synoptic circulation changes noted above, particularly if the model successfully predicts the large-scale controls on the synoptic circulation (i.e. the upper tropospheric temperature gradient and the jet stream location). Consequently, we can have a reasonable level of confidence in the pattern of temperature changes depicted in Figures 9b and 9d, even though the magnitude of the changes may still be open to debate.

This last statement, however, rests on two further assumptions that should also be borne in mind when considering these results. The first, which is common to all numerical climate change experiments, is that the model sensitivity to a doubling of atmospheric CO_2 is correct, and that a GCM 'tuned' to present-day climate will be able to model the changes that would occur in a doubled CO_2 world. We have no choice but to accept this assumption, and how valid it is we will not know until after the fact. The second assumption is that the GCM does an adequate job of predicting the circulation change in a $2xCO_2$ climate. The fact that the model

simulates the present-day circulation more accurately than it does the present-day temperature does not necessarily mean that it will do so in the $2xCO_2$ climate as well. At present, all we can say is that we have more confidence in the model's ability to predict circulation than in its ability to predict accurate grid-point temperatures--based on present-day climate simulations--but that this may change with future GCM developments.

7. SUMMARY AND CONCLUSIONS

Synoptic-scale validation of GCM circulation

The spatial and temporal comparisons of the NMC with the model's component patterns demonstrate that the GISS GCM does simulate the synoptic circulation over the United States. The principal components analysis determines the linear combinations of variables (in this case grid- point sea level pressures) that explain the greatest amount of variance in the data sets, and, as such, the analysis extracts the primary linear modes of spatial variability in sea level pressure. The use of a 13-day running filter ensures the removal, prior to analysis, of most of the variance greater than the synoptic time-scale; thus, the pattern of component loadings can be interpreted in terms of features of the synoptic-scale circulation. The analysis was carried out for the continental United States, and resulted in seven components explaining 82% and 74% of the NMC and GISS data respectively. The correlations between the NMC and the model components reveals a one-to-one match between the first seven components in each set, with the measure of similarity being the average of the component loading correlations and the correlations of the north-south and east-west gradients at each grid point; the model had to match the gradients as well as the spatial patterns in order for a high corrrelation to occur.

Spectral analysis of the component scores shows that each pair of components that are highly correlated spatially, also show high correlations over a 2-12 day temporal bandwidth. Correlations are markedly lower in the 10-31 day bandwidth, which suggests that while individual events develop and dissipate over the same time-scale, the periodicity or repetition varies between the model and the observed data. On the other hand, the power contained in each pair of NMC and GISS components is very similar over the 2-31 day period, showing that each component contributes similar amounts to its data set variance on the monthly time-scale. In other words, the model correctly simulates the location and time-scale of individual synoptic events and correctly simulates the frequency of events in a month, but the timing of events varies between the model and the observed data.

The results presented here are considerably better than those obtained by Crane and Barry (1988) for the Arctic. This may be due in part both to the difference in model resolution--8^{o} x 10^{o} versus 4^{o} x 5^{o} in the present analysis--and to the choice of study area: GCM simulations tend to be weaker at high latitudes, while the continental U.S., where the controlling circulation factors of the upper atmospheric flow are strongly locked in place by the Rockies (although the topography is reduced in the model) and by the baroclinicity of the East Coast, is a region that lends itself to optimal results. Whether equally good results could be obtained for all extra-tropical locations remains to be tested. For the present, however, we can say that the 4^{o}x5^{o} GISS GCM is very effective in simulating the synoptic-scale circulation of the atmosphere over the continental United States.

Synoptic Controls on Temperature and Regional Climate Change

There has been considerable argument in recent years over the issue of possible global warming due to anthropogenic increases in atmospheric greenhouse gasses. The primary tools for assessing the potential impact of this enhanced greenhouse effect are General Circulation Models of the Climate System, and much of the controversy revolves around the reliability of these model predictions. The potential magnitude of the change and the rapidity with which it is likely to occur, however, make this something more than a simple academic debate. If changes of the magnitude suggested by the current generation of GCMs are possible, it becomes vital that we establish the likelihood of such changes as early as we can. Equally important is the fact that if we are to plan for future societal or ecological impacts, then it becomes necessary to make such assessments at the regional scale. This report addressed both of these questions by utilizing a feature of the climate system that the GISS GCM simulates accurately--the synoptic-scale atmospheric circulation--and by using this to assess the regional-scale performance of the GISS $4^{o}x5^{o}$ GCM, and to estimate the regional distribution of the potential CO_2 temperature increase over the United States.

The temperature predictions are derived from a transfer function between atmospheric circulation and grid-point temperature using observational data. These transfer functions are capable of reproducing the temperature field to within +/- $1.5^{o}C$ of the monthly mean over most of the study area in winter, and over about half of the area in summer. The transfer function is then applied to a $1xCO_2$ version of the $4^{o}x5^{o}$ GISS GCM to assess the accuracy of the GCM grid-point temperature simulations, and to a $2xCO_2$ version of the model in order to predict the change in temperature that may occur due to a change in synoptic circulation in a doubled

CO_2 climate. The temperature prediction is independent of the model resolution, providing the model adequately simulates the synoptic circulation. Consequently, the technique describedhere can be applied to any climatic, hydrologic, or ecological parameter; over any size area, as long as there is a strong association between the distribution of that parameter over the region; and the synoptic circulation.

The analysis of the GISS 1xCO_2 climate indicates that the model captures the large-scale temperature distribution, but has significant biases in its individual grid-point temperature calculations. The GCM produces temperatures that are too low over the west coast in both summer and winter, and temperatures that are too high over the north-east in winter, and over the Great Lakes, Florida, and the Gulf coast in summer.

The analysis of the sea level pressure fields in the GISS GCM shows that the model effectively simulates the present day synoptic circulation over the United States, and that the same circulation characteristics are present in the doubled CO_2 climate. The primary modes of the atmospheric circulation do, however, change in intensity and persistence, and in their relative frequency of occurrence. The indication is that, as a result of these differences, the regional distribution of temperature will change, with the U.S. experiencing relatively warmer July temperatures everywhere except the west coast, while in January only the south and east will see a large temperature increase. The central and north-central regions may have little change in winter, and the west coast is cooler in both seasons. The technique assumes that the model sensitivity to a doubling of atmospheric CO_2 is broadly correct, and that the model correctly predicts the large-scale forcing for the synoptic circulation. In this case, the results presented here should provide a reasonable indication of how the CO_2 temperature increase will be distributed across the study area. The technique does not include any large-scale warming due to processes operating at time scales longer than the synoptic scale studied here, although an

estimate of such changes can be obtained from the mean temperature change in the GCM (assuming that the model performance at larger scales is better than at the individual grid-point scale). Finally, some uncertainty in the spatial distribution of the temperature change also exists as the possible effects of differential changes in source air mass characteristics are not included in the analysis.

8. REFERENCES

Barron, E. J. and Washington, W. M. (1984). The role of geographic variables in explaining paleoclimates: Results from Cretaceous climate model sensitivity studies. ***J. Geophys. Res.***, **89**: 1267-1279.

Bates, G. T. and Meehl, G. A. (1986). The effect of CO_2 concentration on the frequency of blocking in a general circulation model coupled to a simple mixed layer ocean model. ***Mon. Wea. Rev.***, **114**: 687-701.

Buell, C. E. (1979). On the physical interpretation of empirical orthogonal functions. Preprints, ***Sixth Conference on Probability and Statistics in Atmospheric Science***, American Meteorological Society, Boston, Mass.: 112-117.

Crane, R.G. (1978). Seasonal variations of sea ice extent in the Davis Strait-Labrador Sea area and relationships with synoptic scale atmospheric circulation. ***Arctic***, **31**: 434-447.

Crane, R.G. (1979). Synoptic controls on the energy budget regime of an ablating fast ice surface. ***Arch. Met. Geoph. Biokl., A***, **28**: 53-70.

Crane, R.G. and Barry, R.G. (1988). Comparison of the MSL synoptic pressure patterns of the Arctic as observed and simulated by the GISS General Circulation Model. ***Met. Atmos. Phys.***, **39**: 169-183.

8. REFERENCES

Cressman, G.P. (1959). An operational objective analysis system. ***Mon. Wea. Rev.***, **87**: 367-374.

Crowley, T. J. (1990). Are there any satisfactory geologic analogs for a future greenhouse warming? ***J. Climate***, **3**: 1282-1292.

Giorgi, F. (1990). Simulation of regional climate using a limited area model nested in a general circulation model. ***J. Climate***, **3**: 941-963.

Grotch, S. L. and MacCracken, M. C. (1991). The use of general circulation models to predict regional climate change. ***J. Climate***, **4**: 286-303.

Hansen, J., Russell, G., Rind, D., Stone, P., Lacis, A., Lebedeff, S., Ruedy, R. and Travis, L. (1983). Efficient three-dimensional global models for climate studies: Models I and II. ***Mon. Wea. Rev.***, **111**: 609-662.

Hansen, J., Lacis, A., Rind, D., Russell, G., Fung, I., Reudy, R. and Lerner, J. (1984). Climate sensitivity analysis of feedback mechanisms. In Hansen, J. and Takahashi, T. (eds) ***Climate Processes and Climate Sensitivity***, Maurice Ewing Series, Vol. 5, AGU, Washington, D.C.: 130-163.

Hewitson, B. C. (1990). ***General Circulation Models: A Validation of Synoptic Circulation***. Unpublished Master's Thesis: 91 pp.

Hewitson, B. C. (1991). ***Regional Climate Changes in the Goddard Institute for Space Studies General Circulation Model***. Unpublished Ph. D. Thesis, the Pennsylvania State University: 170 pp.

Hewitson, B. C. and Crane, R. G. (1992). Regional climates in the GISS GCM: Synoptic-scale circulation. ***J. Climate*** (in press).

8. REFERENCES

Hewitson, B. C. and Crane, R. G. (1992). Greenhouse temperature change over the United States. ***Glob. Plan. Change*** (in press).

Jenne, R.L. (1975). ***Data Sets for Meteorological Research***. NCAR-TN/1A-111, National Center for Atmospheric Research, Boulder, Colorado.

Karl, T. R., Wang, W-C, Schlessinger, M. E., Knight, R. W. and Portman, D. (1990). A method of relating general circulation model simulated climate to the observed local climate. Part I: Seasonal statistics. ***J. Climate***, **3**: 1053-1079.

Klein, W. H. and Klein, J. M. (1984) The synoptic climatology of monthly mean surface temperature in the United States during winter relative to the surrounding 700 mb height field. ***Mon. Wea. Rev.*** , **112**: 433-448.

Klein, W. H. and Klein, J. M. (1986) Synoptic climatology of monthly mean surface temperature in the United States during summer in relation to the surrounding 700 mb height field. ***Mon. Wea. Rev.***, **114**: 1231-1250.

Mitchell, J. F. B. (1990). Greenhouse warming: Is the Mid-Holocene a good analogue. ***J. Climate***, **3**: 1177-1192.

National Academy of Sciences (1986). ***Global Change in the Geosphere-Biosphere: Initial Priorities for an IGBP***, Washington, D.C.

National Research Council (1983). ***Changing Climate***. Report of the Carbon Dioxide Assessment Committee, National Research Council, National Academy Press, Washington, DC.

North, G. R., Bell, T. L., Cahalan, R. F. and Moeng, F. J. (1982). Sampling errors in the estimation of empirical orthogonal functions. ***Mon. Wea. Rev.***, **110**: 699-706.

8. REFERENCES

Overland, J. E. and Preisendorfer, R. W. (1982). A significance test for principal components applied to a cyclone climatology. ***Mon. Wea. Rev.***, **110**: 1-4.

Richman, M.B. (1986). Rotation of principal components. ***J. Climat.***, **6**: 293-335.

Rind, D. (1988). The doubled CO2 climate and the sensitivity of the modeled hydrologic cycle. ***J. Geophys. Res.***, **93**: 5385-5412.

SAS Institute Inc. (1985). ***SAS User's Guide: Statistics***, Version 5 Edition, Cary, NC, SAS Institute Inc.: 956 pp.

Schlesinger, M.E. and Mitchell, J.F.B. (1987). Climate model simulations of the equilibrium climatic response to increased carbon dioxide. ***Rev. Geophys.***, **25**: 760-798.

Volmer, J.P., Deque, M. and Rousselet, D. (1984). EOF analysis of 500 mb geopotential: A comparison between simulation and reality. ***Tellus***, **36**: 336-347.

Walsh, J. E. and Crane, R. G. (1992). A comparison of GCM simulations of Arctic climate. ***Geophy. Res. Let.***, **19**: 29-32..

Wigley, T. M. L., Jones, P. D., Briffa, K. R. and Smith, G. (1990). Obtaining sub-grid-scale information from coarse-resolution general circulation model output. ***J. Geophys. Res.***, **95**: 1943-1953.

Willmott, C.J., Clinton, M.R. and Philpot, W.D. (1985). Small-scale climate maps: A sensitivity analysis of some common assumptions associated with grid-point interpolation and contouring. ***Amer. Cart.***, **12**: 5-16.

Yarnal, B. and Diaz, H.F. (1986). Relationships between extremes of the Southern Oscillation and the winter climate of the Anglo-American Pacific coast. ***J. Climat.***, **6**: 197-219.

9. PUBLICATIONS & CONFERENCE PAPERS SUPPORTED UNDER NAG 5-1133

Publications

Crane, R. G. and Hewitson, B. C. (1991). Regional climates in the GISS GCM. ***AMS Second Conference on Global Change***, Preprint Volume.

Hewitson, B. C. and Crane, R. G. (1992). Regional climates in the GISS GCM: Synoptic-scale circulation. ***J. Climate*** (in press).

Hewitson, B. C. and Crane, R. G. (1992). Regional-scale climate prediction from the GISS GCM. ***Glob. Plan. Change*** (in press)

Hewitson, B. C. (1990). Regional Climates in the GISS GCM: Surface Air Temperature. Submitted to ***Journal of Climate***.

Advanced Degrees Supported under NAG 5-1133

Hewitson, B. C. (1990). ***General Circulation Models: A Validation of Synoptic Circulation***. Unpublished Master's Thesis, the Pennsylvania State University: 91 pp.

Hewitson, B. C. (1991). ***Regional Climate Changes in the Goddard Institute for Space Studies General Circulation Model***. Unpublished Ph.D. Thesis, the Pennsylvania State University: 170 pp.

Palecki, M. A. (1991). ***Variability of 500-mb Geopotential Heights in a General Circulation Model and the Projection of Regional Greenhouse Effect Climate Change***. Unpublished Ph.D. Thesis, the Pennsylvania State University: 239 pp.